

Crystal Structure of Human Ubiquitous Mitochondrial Creatine Kinase

Michael Eder,^{1,2} Karin Fritz-Wolf,² Wolfgang Kabsch,^{2*} Theo Wallimann,¹ and Uwe Schlattner¹

¹*Institute of Cell Biology, Swiss Federal Institute of Technology (ETH), Zurich, Switzerland*

²*Department of Biophysics, Max-Planck Institute for Medical Research, Heidelberg, Germany*

ABSTRACT Creatine kinase (CK), catalyzing the reversible trans-phosphorylation between ATP and creatine, plays a key role in the energy metabolism of cells with high and fluctuating energy requirements. We have solved the X-ray structure of octameric human ubiquitous mitochondrial CK (uMtCK) at 2.7 Å resolution, representing the first human CK structure. The structure is very similar to the previously determined structure of sarcomeric mitochondrial CK (sMtCK). The cuboidal octamer has 422 point group symmetry with four dimers arranged along the fourfold axis and a central channel of ~20 Å diameter, which extends through the whole octamer. Structural differences with respect to sMtCK are found in isoform-specific regions important for octamer formation and membrane binding. Octameric uMtCK is stabilized by numerous additional polar interactions between the N-termini of neighboring dimers, which extend into the central channel and form clamp-like structures, and by a pair of salt bridges in the hydrophobic interaction patch. The five C-terminal residues of uMtCK, carrying positive charges likely to be involved in phospholipid-binding, are poorly defined by electron density, indicating a more flexible region than the corresponding one in sMtCK. The structural differences between uMtCK and sMtCK are consistent with biochemical studies on octamer stability and membrane binding of the two isoforms. *Proteins* 2000;39:216–225. © 2000 Wiley-Liss, Inc.

Key words: guanidino kinases; oligomeric protein; cellular energy metabolism; membrane binding

INTRODUCTION

Creatine kinase (CK) has evolved to cope with high and fluctuating energy demands of very specialized cells such as muscle fibers, neurons, or sperm cells. By catalyzing the reversible trans-phosphorylation between ATP and creatine (Cr), CK can build up a large pool of the easily diffusible “high energy” intermediate phosphocreatine (PCr) at sites of ATP generation. Vice versa, PCr is used by CK to restore ATP levels at sites of energy demand. This cellular energy buffer and transport system, referred to as CK/PCr shuttle or circuit (reviewed in Wallimann et al.,¹ Wyss et al.,² Schlattner et al.³), relies on the presence of different CK isoforms in cytosol (BB-, MB-, and MM-CK)

and mitochondria (MtCK). Vertebrate genomes code for two distinct and tissue-specific MtCK isoforms sharing 82–85% amino acid sequence identity:⁴ ubiquitous MtCK (uMtCK), found in brain and several other organs, and sarcomeric MtCK (sMtCK), strictly confined to muscle tissue. While detailed information about uMtCK is still scarce, sMtCK from various organisms has been extensively characterized (reviewed in Wyss et al.,² Schlattner et al.,³ Stachowiak et al.⁵).

MtCK is located in the mitochondrial cristae and in the peripheral intermembrane space. Both MtCK isoforms are basic proteins, which form dimeric as well as highly ordered octameric structures with a molecular weight of about 86 and 340 kD, respectively.^{2,6} In contrast to the invariably dimeric cytosolic CK, the octamer is the predominant form of MtCK in vivo.^{7,8} It was shown in vitro that only the MtCK octamer strongly binds to phospholipid membranes and is able to crosslink two membranes.^{9,10} In vivo, MtCK is found in the so-called mitochondrial contact sites, where it interacts functionally and possibly also structurally with the adenylate translocator (ANT) in the outer membrane¹¹ and mitochondrial porin (VDAC) in the inner membrane (reviewed in Stachowiak et al.⁵). The direct transphosphorylation of intramitochondrially produced ATP into PCr is probably the primary function of MtCK with regard to the CK/PCr-circuit. Recently, an additional role of MtCK in regulating the Ca²⁺-induced mitochondrial permeability transition pore (PTP) has been proposed. PTP, which most probably includes ANT and VDAC, plays an important role in the execution pathway of apoptosis (reviewed in Crompton¹²). Experiments with isolated mitochondria have demonstrated that the presence of active octameric MtCK is able to prevent or at least delay opening of PTP.¹³ Some studies suggest that only the membrane-bound, octameric form of MtCK is functional in the proposed CK/PCr-circuit or as a regulator of PTP.^{13,14} The octamer/dimer ratio of sMtCK may therefore be of

Abbreviations: ANT, adenylate translocator; BB-, MB-, MM-CK, cytosolic CK isoforms; CK, creatine kinase; MtCK, mitochondrial CK; Cr, creatine; PTP, permeability transition pore; sMtCK, sarcomeric MtCK; SPR, surface plasmon resonance; uMtCK, ubiquitous MtCK; VDAC, voltage-dependent anion channel (mitochondrial porin).

Grant sponsor: ETH graduate training; Grant sponsor: Swiss National Science Foundation; Grant number: 3100-5082.97.

*Correspondence to: Wolfgang Kabsch, Max-Planck Institute for Medical Research, Department of Biophysics, Jahnstr. 29, D-69120 Heidelberg, Germany. E-mail: kabsch@mpimf-heidelberg.mpg.de

Received 20 August 1999; Accepted 20 December 1999

physiological relevance as a medium or long-term regulator of the MtCK system.^{2,15} In fact, increased sMtCK dimer levels were detected in animal models of ischemic heart¹⁶ and natural dimerization triggers may therefore include peroxynitrite or reactive oxygen species and other radicals known to inhibit CK activity and to destabilize the MtCK octamer.^{16–18}

Recent studies on ubiquitous and sarcomeric MtCK isoforms revealed striking differences in octamer stability and membrane binding (Schlattner and Wallimann, unpublished data). Octamer dissociation rates of uMtCK were ≈ 30 -fold slower than for sMtCKs and octamer/dimer ratios at thermodynamic equilibrium indicated higher stability of uMtCK. Moreover, detailed studies on the temperature dependence of octamer stability indicated the presence of additional polar interactions at the dimer/dimer interface of human uMtCK. Association rates and affinity constants in binding to artificial model membranes, as determined by surface plasmon resonance (SPR) techniques, were slightly higher for sMtCK, whereas uMtCK could occupy a higher number of binding sites at the vesicle surface.

Human uMtCK, like the CK/PCr system in general, is also relevant for human health and disease. Cr supplementation has gained particular interest as a potential adjuvant therapy for neuromuscular or neurodegenerative diseases.¹⁹ A common denominator of such diseases is a disturbed mitochondrial energy metabolism, including free radical generation and mitochondrial permeability transition.²⁰ Thus, Cr supplementation might improve mitochondrial energy status and decrease opening probability of PTP by stabilizing octameric uMtCK. On the other hand, overexpression of uMtCK is found in malignant tumors with especially poor prognosis.²¹ Here, the PCr/CK system may maintain favorable energetics for cancer growth and inhibit apoptotic elimination of cancer cells. Such a function is supported by the strong anti-cancer effect of certain inhibitory Cr-analogs.²²

The overall structure of sMtCK has been well characterized by 2D-crystals,^{6,23} and chicken sMtCK, co-crystallized with ATP, was the first CK X-ray structure solved.²⁴ Together with the recently published molecular structures of rabbit MM-CK²⁵ and chicken BB-CK,²⁶ it represents the “open” conformation of the enzyme. In addition, a “closed” transition state structure has been determined with monomeric arginine kinase from horseshoe crab,²⁷ an enzyme that is highly homologous to CK (both belong to the guanidino kinase family). With the structure of uMtCK, described in this paper, all homo-oligomeric isoforms of vertebrate CK will be known. This provides a structural basis for rationalizing isoform-specific properties, which is expected also to help clarifying CK's role in different pathologies.

MATERIALS AND METHODS

Cloning, Expression, and Purification

Cloning of full-length cDNA for human ubiquitous MtCK (uMtCK, GenBank accession J04469) has been described previously.²⁸ The cDNA contains a 5'-

sequence coding for a N-terminal signal peptide, which had to be removed by PCR to obtain the mature protein. It should be noted that the engineered cDNA of human uMtCK is coding for an additional alanine yielding a N-terminal sequence AASE. . . , in contrast to the SwissProt entry P12532. Consequently, the residue numbering of human uMtCK, as used in this paper, coincides with that of the sMtCK isoform. PCR and subcloning, yielding expression vector pUS04, as well as expression and purification of mature human uMtCK, was performed after Furter et al.²⁹ with minor modifications. Remaining impurities were eliminated using a HiPrep Sephacryl S 300-16/60 column (Pharmacia, Dübendorf, Switzerland). The final preparation of uMtCK used in crystallization setups was $> 99\%$ pure as judged by standard 12% SDS-PAGE (data not shown) and had a specific activity of ~ 105 U/mg protein in the reverse reaction (ATP production). Protein concentration was determined with the Bio-Rad reagent using bovine serum albumin as a standard.³⁰ Enzymatic activity of purified uMtCK as well as of redissolved uMtCK crystals were determined by standard assay methods with a coupled enzyme test in the photometer.³¹

Crystallization

For crystallization, purified human uMtCK was transferred into a low salt buffer system (25 mM sodium phosphate, 2 mM β -mercaptoethanol, 0.2 mM EDTA, pH 6.75) by a fast desalting Sephadex G25 M column (Pharmacia PD-10) and concentrated to 4–5 mg/ml by ultrafiltration (Centricon 30, Grace, Beverly, MA). Similar to the human sarcomeric sMtCK isoform (M. Eder, unpublished results), human uMtCK displays a relatively low solubility in low salt buffers around pH 7, which allows the protein to be concentrated to a maximum of only ~ 5 mg/ml without precipitation. Single batch crystallization leaving 50 μ l of the above protein solution in a closed Eppendorf tube at 4°C for 5–7 days yielded large crystals of human uMtCK with dimensions of up to $2.5 \times 2 \times 1.5$ mm. Size and quality of the crystals were improved by filtration of the protein through 0.2 μ m membranes prior to crystallization and by microseeding. Crystals of human uMtCK belong to spacegroup P 2₁ with cell dimensions of $a = 91.81$ Å, $b = 125.87$ Å, $c = 212.07$ Å, $\beta = 96.71^\circ$ and contain one octamer in the asymmetric unit. The resulting Matthews coefficient is $V_M = 3.5$ which corresponds to a calculated solvent content of 65%. Gel filtration chromatography of redissolved human uMtCK crystals confirmed that the octameric form of the protein has been crystallized (data not shown).

Data collection

Diffraction data were recorded by the rotation method and processed with the program package XDS.^{32,33} A complete dataset to 2.7 Å was collected from 5 crystals at 4°C using CuK α radiation from a rotating anode X-ray generator (GX-18, Elliot/Enraf-Nonius, Delft, operated at 35 kV/50 mA; focussed by Franks double-mirror optics; detector: X 100, Siemens/Nicolet, Madison, WI; crystal to

TABLE I. Data Collection Statistics

λ (Å)	1.5418
Temperature (K)	277
Number of crystals	5
Spacegroup	P 2 ₁
Unit cell (Å)	a = 91.81, b = 125.87, c = 212.07, β = 96.71
Resolution (Å)	50–2.7
Last shell (Å)	2.8–2.7
Measured reflections	616,668/(43256) ^a
Unique reflections	130,945/(13429) ^a
Completeness [%]	99.4/(99.1) ^a
$\langle I/\sigma \rangle$	11.1/(2.7) ^a
Redundancy	4.7/(3.2) ^a
R_{sym} [%] ^b	9.2/(31.3) ^a
$R_{\text{mrgd-F}}$ [%] ^c	8.3/(20.3) ^a

^aValues in parentheses are given for the highest resolution shell.

^b $R_{\text{sym}} = \sum_h \sum_i |I_{hi} - I_h| / \sum_h \sum_i I_{hi}$ where h are unique reflection indices and I_{hi} are the intensities of symmetry equivalent reflections giving a mean value of I_h .

^c $R_{\text{mrgd-F}}$ as defined by Diederichs and Karplus⁵¹ is a quality measure of the reduced structure factor amplitudes.

detector distance: 16 cm; rotation/image: 0.0417° or 0.0833°). Data collection statistics are summarized in Table I.

Model Building and Refinement

An initial solution was found by molecular replacement³⁴ using the coordinates of octameric chicken sMtCK (PDB entry 1crk²⁴), which has 82% of the residues in common with human uMtCK.⁴ Rotation and translation function analysis was carried out with CNS³⁵, using data from 15–4.0 Å resolution. The initial σ_A -weighted $2F_o - F_c$ electron density map³⁸ clearly defined the octamer in the asymmetric unit.

The initial free R-factor of the model dropped from 47.0% to 37.7% after rigid body minimization (B-factors fixed at 20 Å² using data from 100–3.6 Å. The final free R-factor is 21.9% after several rounds of model correction (Quanta97, MSI, San Diego, CA) and refinement, using all data between 100–2.7 Å with no σ cutoff. The quality of the final model was evaluated with Procheck⁴² and built-in features of CNS.

Refinement was performed with CNS 0.5,³⁵ leaving out 5% of the reflections for the calculation of the free R-factor.³⁶ The geometry of the model was restrained to the standard parameters of Engh & Huber.³⁷ Noncrystallographic symmetry (NCS) restraints were applied to increase the effective data to parameter ratio. In later refinement stages, NCS restraints were slightly relaxed by excluding residues 1–8, 60–66, 111–113, 148–155, 293–305, 316–326, and 355–379. Water molecules were assigned to peaks > 4.5 σ in the σ_A -weighted $F_o - F_c$ maps, if at least one potential hydrogen-bonding partner was available. Coordinates and measured structure factor amplitudes of human uMtCK have been deposited in the Brookhaven Protein Data Bank (PDB, accession code 1qk1 and r1qk1sf, respectively).

TABLE II. Refinement Statistics

Number of reflections used in refinement	124,397
Number of reflections used for Rfree	6,548
Resolution range	50.0–2.7
R_{cryst} (%) ^a	19.5
R_{free} (%) ^b	21.9
Content of the model	
Protein atoms (non-hydrogen)	24,280
Solvent molecules	293
Phosphate ions	8
B-factor model	Restrained individual
Mean B-factor (protein)	45.02
Mean B-factor (water)	31.17
Rmsd	
Bond distances (Å)	0.011
Bond angles (°)	1.6
Improvers (°)	23.6
Dihedrals (°)	0.94

^a $R_{\text{cryst}} = \sum |F_{\text{obs}} - F_{\text{model}}| / \sum F_{\text{obs}}$ where F_{obs} and F_{model} are observed and atomic model structure factor amplitudes, respectively.

^bR-factor calculated for 5% of randomly chosen reflections which were excluded from the refinement.

RESULTS

Quality of the Model

The final model of human uMtCK has a free R-factor of 21.9% ($R_{\text{cryst}} = 19.5\%$) including all data up to 2.7 Å resolution. Refinement and model statistics are summarized in Table II. The model includes all residues of the octamer, one phosphate-ion per monomer, and 293 water molecules. The residues of a highly flexible loop (316–326) and the last five residues at the C-terminus were included in the model, although none of the monomers displayed significant electron density for these residues. Weak density was also found for the four N-terminal residues and for some side chains of a second flexible loop (residues 61–65). The flexibility of these regions is also observed in the crystal structures of chicken sMtCK,²⁴ rabbit MMCK,²⁵ and chicken BB-CK,²⁶ which have all been determined in the “open” unliganded form.

The model conforms well with standard geometry: 88.8% of all non-glycine and non-proline residues have main-chain torsion angles in the most favorable region of the Ramachandran plot,⁴³ 9.7% are in additionally allowed, and 1.3% in generously allowed regions. Only five residues (Glu4 (B), Thr377 (C), Ala324 (D), Thr325 (F), and His376 (H)) are in the disallowed region of the Ramachandran plot, as defined by Procheck.⁴² They all belong to flexible regions (1–5, 316–326, 375–379) without significant density. The refined model exhibits good stereochemistry with standard deviations of 0.010 Å (bonds) and 1.6° (angles) from standard values.³⁷

OVERALL STRUCTURE

Human uMtCK has been crystallized in its octameric form, which represents its predominant oligomeric state in vivo as well as in vitro.^{3,15} The octamer displays 422 point group symmetry and is assembled from four elongated “banana-shaped” dimers arranged around its fourfold axis.

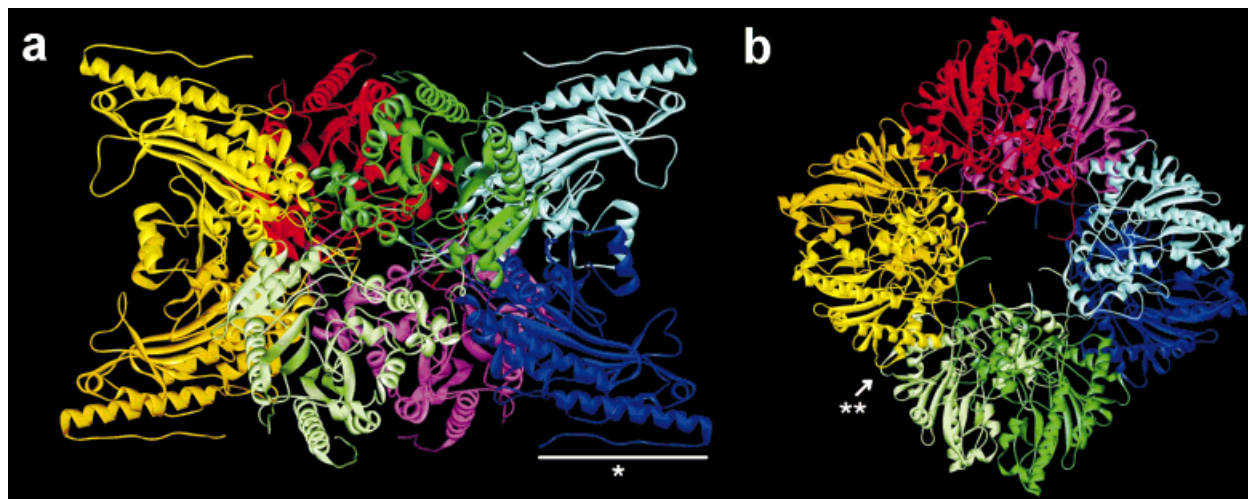


Fig. 1. Cartoon representation of a cube-like octamer of human uMtCK. The monomers are drawn in yellow (chain A), orange (E), cyan (B), blue (F), red (C), magenta (G), dark green (D), and light green (H). **a**: Side view of the octamer along one of its twofold axes. Four dimers are arranged around the vertical fourfold axis. Membrane binding occurs via the identical top or bottom faces. At the bottom side of the octamer, one of

the four putative C-terminal membrane-binding regions is indicated (*). **b**: Top view along the fourfold axis of the octamer. The N-termini of the monomers, protruding into a central channel with a diameter of ~ 20 Å, intertwine with N-termini of neighboring dimers. One of the four dimer/dimer interfaces is indicated (**). The figure was prepared with WebLab-Viewer Lite V. 3.1 (MSI, San Diego, CA).

The overall dimensions of the octamer are approximately $105 \times 105 \times 86$ Å (Fig. 1). It was shown that the top and bottom faces, perpendicular to the fourfold octamer axis, bind to the mitochondrial membranes.^{9,23} A central “channel” of ~ 20 Å diameter extends through the entire octamer along its fourfold axis and the N-termini of the monomers protrude into this central channel mediating contact to neighboring dimers (Fig. 1b). The monomers are named A–H; the dimers constituting the four stable building blocks of the octamer are A : E, B : F, C : G, and D : H, respectively.

Chain Fold

Differences between the eight crystallographically independent monomers of human uMtCK are minimal and mainly restricted to flexible, solvent accessible regions comprising the N-terminus (residues 1–5), the loop 316–326, and the C-terminus (residues 375–379). Excluding these residues, pairwise superposition of the monomers yields rms deviations as small as 0.18–0.27 Å for C_{α} -atoms and 0.37–0.52 Å for all atoms (358 residues per monomer included).

uMtCK monomers consist of a small N-terminal domain (residues 1–95) and a larger C-terminal domain (residues 120–379) connected by a long linker region (residues 96–119). The N-terminal domain contains six α -helices. The large domain comprises an eight-stranded antiparallel β -sheet flanked by seven α -helices. Figure 2 depicts the chain fold and the secondary structure assignment as obtained with DSSP.⁴⁴

The fold of the monomers follows closely that described for other CK isoenzymes (chicken sMtCK: PDB code 1crk²⁴, cytosolic muscle-type MM-CK: PDB code 2crk²⁵, cytosolic brain-type BB-CK: PDB code 1qh4²⁶) and horse-shoe crab arginine kinase (PDB code 1bg0²⁷). Superposi-

tion of a human uMtCK monomer with a monomer of chicken cytosolic BB-CK or rabbit cytosolic MM-CK results in rms deviations of 0.65 Å (356 C_{α} -pairs) and 0.71 Å (353 C_{α} -pairs), respectively. The similarity of human uMtCK with that of chicken sMtCK is illustrated in Figure 3. Here, the rms deviation is 0.55 Å for 356 C_{α} -pairs, leaving out the N-terminus (1–8), the flexible loop (317–326) and the C-terminus (375–379).

Monomer/Monomer Interface

All CK isoforms are known to form very stable dimers, which can be disintegrated into monomers only under drastic conditions along with partial unfolding of the monomer.⁴⁵ In the case of human uMtCK, dimer formation reduces the sum of the solvent-accessible surface areas of the monomers by $\sim 2,200$ Å², as calculated by DSSP.⁴⁴ This value is comparable to that of chicken sMtCK (2,200–2,690 Å²; depending on the chosen dimer), but smaller than that of cytosolic BB-CK (3,702 Å²; ²⁶). In addition to the hydrophobic interface regions from solvent exposure, 12 hydrogen-bonded interactions between the monomers can be identified in the structure, which further stabilize the dimer (Table III). Although dimer formation is a common feature of all CK isoforms, the hydrogen-bond forming residues are predominantly isoenzyme-specific and only Asp57, Arg143, Arg148, and Asp205 are conserved in the entire CK family.

Dimer/Dimer Interface

The ability to form octamers is a unique feature of mitochondrial isoforms of CK. In human uMtCK, the octamer is stabilized by numerous polar and electrostatic interactions between contacting dimers (Table IV). Key residues involved in these interactions are shown in Figure 4a. At the N-terminus of uMtCK, residues 1–10

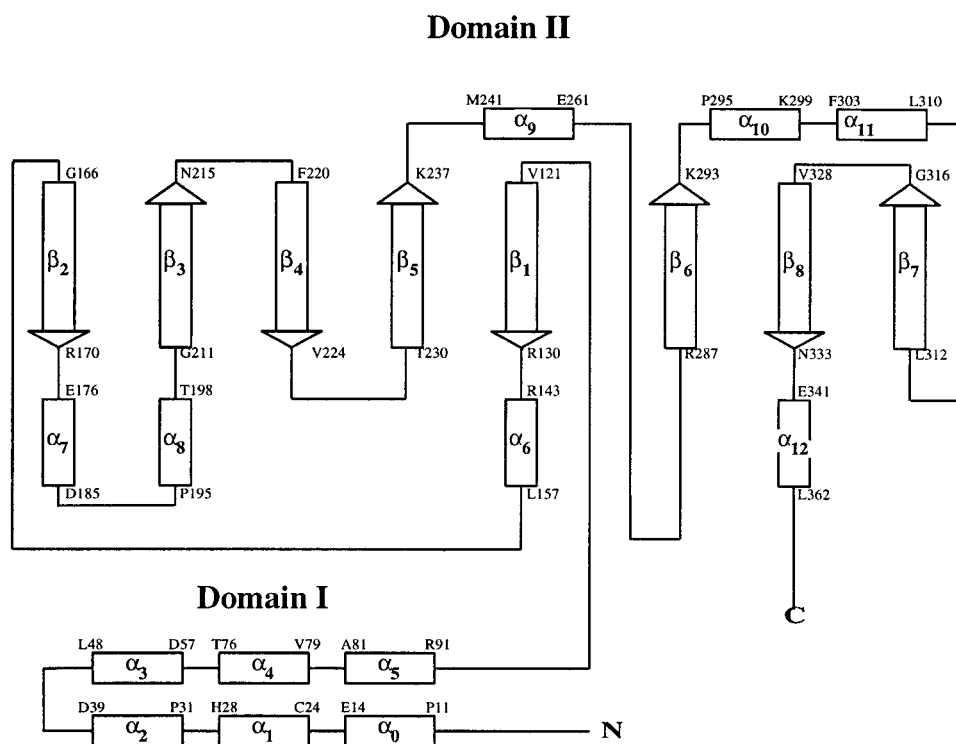


Fig. 2. Schematic representation of the secondary structure of human uMtCK as provided by DSSP.⁴⁴ First and last residues in the secondary structure elements are specified using single-letter amino acid code. α -helix numbering starts with α_0 to be consistent with the secondary structure assignment of chicken sMtCK, which starts with a short 3_{10} -helix.²⁴

extend from the monomer core and intertwine with the N-terminus of a neighboring dimer (Fig. 1b and 4b). This clamp-like interaction involves residues Arg6, Arg 7, and Tyr9 forming salt bridges or hydrogen-bonds with residues of the contacting dimer. A second electrostatic contact region comprises residues 148, 151, and 155. Arg151, which is specific to ubiquitous MtCKs, forms a salt bridge with either Glu148 (conserved in all MtCKs) or Asp155 (only in ubiquitous MtCKs) of the neighboring dimer (Fig. 4c).

The calculated contact surface of uMtCK between two dimers in the octamer is $\sim 1,900 \text{ \AA}^2$, which is considerably larger than that of chicken sMtCK ($\sim 900 \text{ \AA}^2$). This indicates a tight interaction between the dimers with a significant contribution of hydrophobic interactions. In fact, numerous aromatic or hydrophobic residues, including Tyr9, Pro10, Pro11, Tyr15, Pro31, and Trp264, are located at the edge of the contact area, thus shielding the central electrostatic interactions (Arg151/Glu148 and Arg151/Asp155 salt bridges) from solvent (Fig. 4a,c). Trp264, which is conserved in all mitochondrial CKs, is a key residue for octamer stability as demonstrated by site-directed mutagenesis in chicken sMtCK.⁴⁶

DISCUSSION

The 3-dimensional structure of octameric human uMtCK, solved at a resolution of 2.7 \AA , represents the first CK structure of human origin. The octamers display all the

TABLE III. Polar Interactions Across the Monomer-Monomer Interfaces in uMtCK

Monomer I ^a				Monomer II ^a		
Tyr	9	OH	\leftrightarrow	Glu	148	COO ⁻
Ala	13	CO	\leftrightarrow	Arg	147	NH ₂
Glu	14	COO ⁻	\leftrightarrow	Thr	142	OH
Tyr	15	CO	\leftrightarrow	Arg	147	NH ₂
Lys	20	NH ₂	\leftrightarrow	Ser	172	CO
Asp	57	COO ⁻	\leftrightarrow	Asp	205	NH
Thr	142	OH	\leftrightarrow	Glu	14	COO ⁻
Arg	143	NH ₂	\leftrightarrow	Glu	14	CO
Arg	147	NH ₂	\leftrightarrow	Tyr	15	CO
Glu	148	COO ⁻	\leftrightarrow	Tyr	9	OH
Ser	172	CO	\leftrightarrow	Lys	20	NH ₂
Asp	205	NH	\leftrightarrow	Asp	57	COO ⁻

^aMonomer I and II represent two monomers building a proper dimer of uMtCK. Amino acid, residue number, and functional group are given. A cutoff distance of 3.2 \AA was used to identify hydrogen-bonded interactions between the monomers.

general structural features already known for chicken sMtCK, such as internal 422-point group symmetry,⁶ the presence of a central "channel" with a diameter of $\sim 20 \text{ \AA}$ running through the whole octamer along its fourfold axis, and C-termini properly exposed to the fourfold faces to mediate membrane binding. Except for the N-terminal residues 1–9 the overall fold of human uMtCK is very similar to all CK structures solved so far.^{24–26} In particu-

TABLE IV. Polar and Charged Interactions Across the Dimer-Dimer Interfaces in Human uMtCK

Dimer II ^a				Dimer I ^a				Dimer III ^a			
Salt bridges											
Asp	39 ^c	COO ⁻	↔	Arg	6 ^b	NH2					
Glu	145 ^b	COO ⁻	↔	Arg	7 ^b	NH2					
Arg	6 ^c	NH2	↔	Asp	39 ^b	COO ⁻					
				Glu	145 ^b	COO ⁻	↔	Arg	7 ^b	NH2	
				Glu	148 ^b	COO ⁻	↔	Arg	151 ^c	NH2	
				Arg	151 ^b	NH2	↔	Asp	155 ^c	COO ⁻	
				Arg	6 ^c	NH2	↔	Asp	39 ^b	COO ⁻	
				Arg	7 ^c	NH2	↔	Glu	145 ^c	COO ⁻	
Arg	7 ^c	NH2	↔	Glu	145 ^c	COO ⁻					
Glu	148 ^b	COO ⁻	↔	Arg	151 ^c	NH2					
Arg	151 ^b	NH2	↔	Asp	155 ^c	COO ⁻					
Polar interactions											
Tyr	9 ^c	NH	↔	Arg	7 ^b	CO					
Arg	6 ^c	NH2	↔	Tyr	9 ^b	CO					
Arg	7 ^c	CO	↔	Tyr	9 ^b	NH					
Gly	263^b	CO	↔	Ser	12^b	OH					
				Ala	140 ^b	CO	↔	Arg	7 ^b	NH2	
				Arg	6 ^c	NH2	↔	Tyr	9 ^b	CO	
				Arg	7 ^c	CO	↔	Tyr	9 ^b	NH	
				Arg	7 ^c	NH2	↔	Ala	140 ^c	CO	
				Tyr	9 ^c	CO	↔	Arg	6 ^b	NH2	
				Tyr	9 ^c	NH	↔	Arg	7 ^b	CO	
				Ser	12^c	OH	↔	Gly	263^c	CO	
Arg	7 ^c	NH2	↔	Thr	44 ^c	CO					
Ser	12 ^c	OH	↔	Gly	263 ^c	CO					

^aEach dimer (termed Dimer I) in the uMtCK octamer is in contact with two neighboring dimers (Dimer II and III). Amino acid, residue number, and functional group of interacting residues are given. A cutoff distance of 3.2 Å was used to identify charged and polar interactions between the dimers. Polar interactions also found in chicken sMtCK are indicated in bold face.

^bResidue belongs to chain A, B, C, or D.

^cResidue belongs to chain E, F, G, or H.

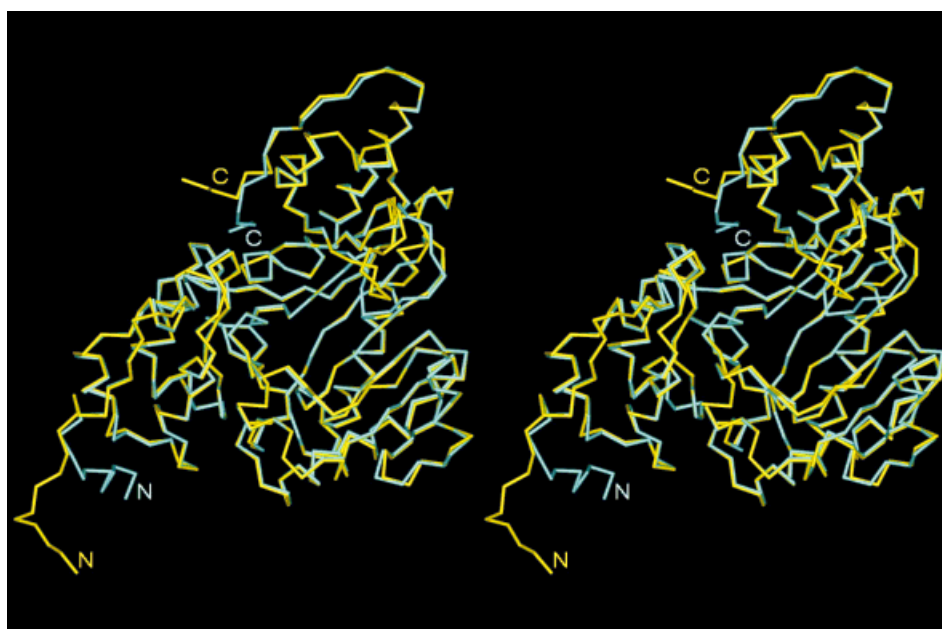


Fig. 3. Superposition of human uMtCK (yellow) with chicken sMtCK (cyan). C_α-traces of superimposed human uMtCK and chicken sMtCK monomers illustrating the structural differences are drawn in stereo. The figure was prepared with WebLabViewer Lite V. 3.1 (MSI, San Diego, CA).

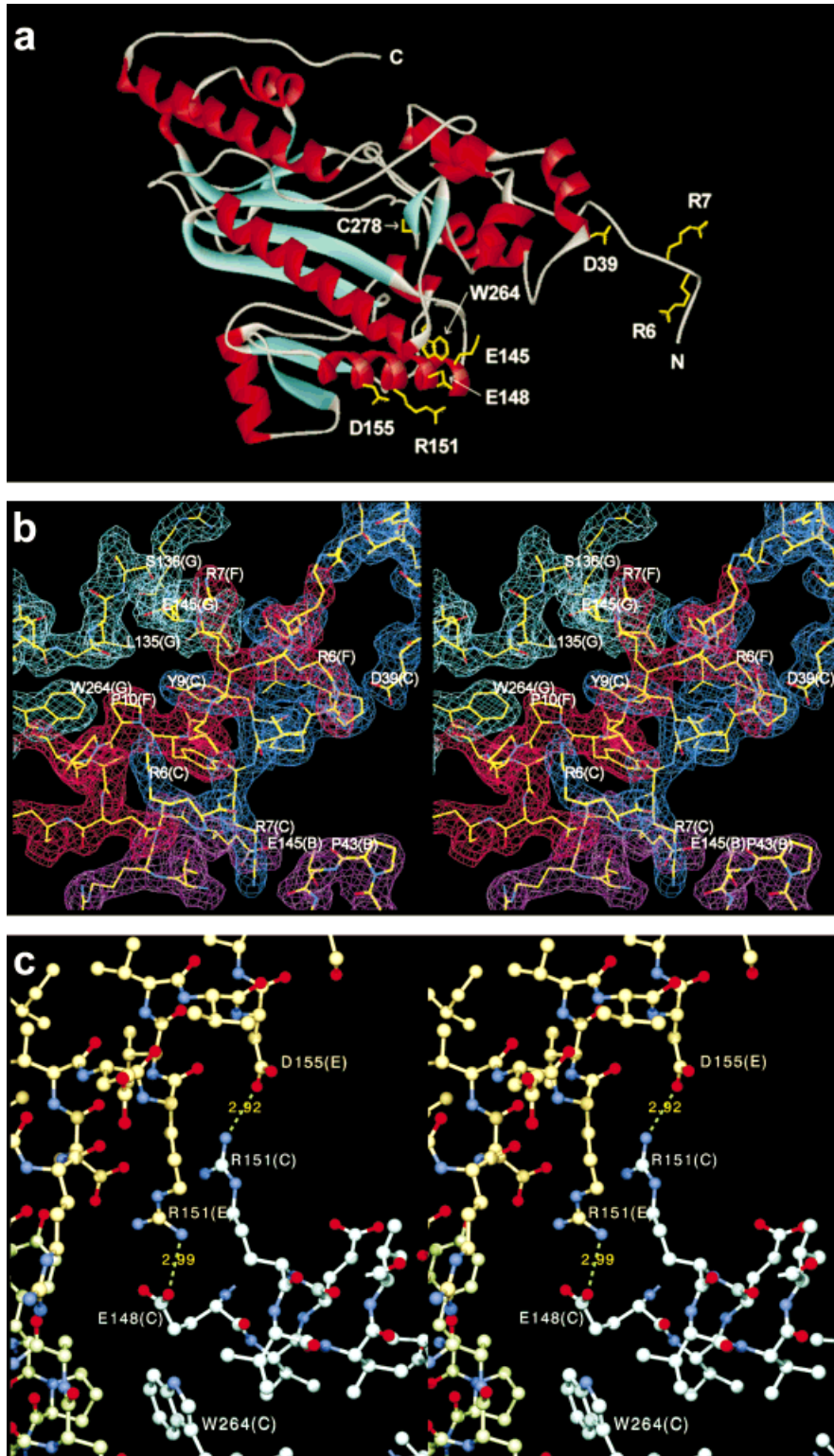


Fig. 4. Dimer/dimer interface of human uMtCK. **a**: Cartoon representation of a monomer viewed from the "back side" (opposite to the active site view, see Figure 3). Key residues (yellow), α -helices (red) and β -sheets (cyan) are indicated. Note that C278 marks the active site. **b**: Stereo view of the final σ_A -weighted $2F_o - F_o$ map at 2.7 Å with phases from the refined model, showing the dense interaction network between adjacent dimers in the N-terminal region. The contact between the neighboring dimers B:F (magenta/red) and C:G (blue/cyan) involves N-termini of monomers F and C (see Fig. 1b). The maps are contoured at 1.5σ and the model is drawn in a smooth stick representation using standard CPK colors. Residue labels include a chain identifier in parentheses. **c**: Stereo view of the salt bridge pairs Arg151/Glu148 and Arg151/Asp155 in the center of the dimer/dimer contact surface. The model is depicted in a ball-and-stick representation and carbon atoms are colored-shaded in yellow (chain E), cyan (chain C), or light green (chain A); all other atoms are in standard CPK colors. Residue labels include a chain identifier in parentheses. Figure 4a was generated with WebLabViewer Lite V. 3.1 (MSI, San Diego, CA), Figure 4b with the program O⁵² and Figure 4c with Swiss-PDBViewer V. 3.1 (N. Guex, Glaxo Wellcome Experimental Research) and subsequent rendering with POVray V. 3.1 (<http://www.povray.org>).

lar, the similarity includes the strictly conserved residues Trp206 and Pro207, which are connected by a cis-peptide link, and the negatively charged cluster Glu226, Glu227, and Asp228, which were recently shown by site-directed mutagenesis to be essential for catalytic activity (Eder et

al., unpublished data). However, since no suitable CK crystals could be grown in the presence of both substrates or the transition state analog complex (MgADP, NO_3^- and creatine⁴⁷), the structures of all of these enzymes, including human uMtCK, represent the unliganded "open" state.

They give no details about the substrate binding mode in the ternary “active” enzyme complex.

As for the other CK structures, we found the loop 316–326 and the side chains of the loop 61–65 disordered. Both loops have been proposed to move towards the active site during catalysis,²⁴ an assumption that has been confirmed recently by the crystal structure of arginine kinase (another member of the guanidino kinase family) in the transition state.²⁷ In this structure, representing the “closed” conformation of the enzyme, the loops corresponding to 61–65 and 316–326 in uMtCK participate directly in binding of the guanidino substrate.

Recent studies on human ubiquitous and sarcomeric MtCK, as well as on chicken sarcomeric MtCK, revealed strikingly higher octamer stability of uMtCK as compared to sMtCK and a different membrane binding behavior (Schlattner and Wallimann, unpublished data). The largest difference between the structures of human uMtCK and chicken sMtCK can be seen at the N-terminus, where the first nine residues accommodate a completely different conformation (Fig. 3). The main chain of human uMtCK extends from the monomer core intertwining with an N-terminus of a contacting dimer with Arg6 and Arg7 forming extensive contacts with this neighboring dimer (Fig. 4b; Table IV), whereas Arg6 of chicken sMtCK interacts with residues of its own monomer and Lys7 does not form any specific contacts with residues of other chains.

The second key region involves Arg151, which is specific to uMtCKs.⁴ In human uMtCK, two Arg151 side chains originating from different monomers are located in the center of the dimer/dimer interface, each of them forming a salt bridge pair (Fig. 4c). A total of 12 hydrogen-bonded or charged interactions stabilizes the dimer/dimer interface of human uMtCK, and only one out of these 12 polar interactions are also found in sMtCK (see also Table IV). These polar interactions, which add to the mainly hydrophobic dimer/dimer interaction patch, clearly increase stability of uMtCK octamers. Interestingly, another mitochondrial CK forming stable octamers has been described by Ellington and co-workers in the polychaete *Chaetopterus variopedatus*.⁴⁸ A sequence comparison with human uMtCK reveals an arginine at a position corresponding to Arg151 in uMtCK and two negatively charged residues corresponding to Glu148 and Asp155 in uMtCK. Thus, a salt bridge pair similar to uMtCK is likely to be present at the dimer/dimer interface of *Chaetopterus* MtCK.

A further reason for increased octamer stability of human uMtCK could be due to additional hydrophobic interactions across the interface. This is indicated by a roughly twofold increased interface area in human uMtCK as compared to chicken sMtCK. Taken together, the additional interactions found in the crystal structure of human uMtCK are in perfect agreement with the properties of uMtCK octamers determined by biophysical methods (Schlattner and Wallimann, unpublished data).

The current model on MtCK functioning assumes that octamers, in contrast to dimers, are able to interact with the membrane proteins adenine translocator and porin, to

maintain creatine-stimulated oxidative phosphorylation¹⁴ and to regulate the mitochondrial permeability transition.¹² Therefore, increased octamer stability of uMtCK could be an adaptation to provide better resistance against energy failure or apoptosis in pathological situations. This would also explain why uMtCK overexpressing tumors are characterized by a very poor prognosis.²¹

Membrane binding of MtCK is directly related to the octamer/dimer ratio, since dimers of MtCKs bind only weakly to the mitochondrial membranes.^{5,9,10} In contrast to the structure of chicken sMtCK, the last five residues at the C-terminus (375–379) of human uMtCK were completely disordered. We suggest that the increased flexibility of the C-terminus, located at the fourfold faces of the octamer, could be used as a highly adaptive membrane anchor, possibly not only via interactions of positively charged residues with the negatively charged head groups of the phospholipids, but also by inserting in part into the mitochondrial membranes. In fact, the predominantly hydrophobic residues 370–375 of MtCKs are well suited for the proposed membrane insertion.³ However, it is still a matter of debate whether the octamer only binds to the membrane surface⁴⁹ or penetrates partially into the lipid bilayer.^{9,50}

The slower association rate and lower affinity of human uMtCK to model membranes, as determined by in vitro SPR experiments (Schlattner and Wallimann, unpublished data), suggest a different membrane interaction mode for this isoform. Clearly, an insertion into the membrane would require some rearrangements in the lipid bilayer, slowing down the binding process. On the other hand, one would expect that uMtCK, once anchored in the membrane, exhibits a tighter binding to the membranes, an assumption which could not be proven by these SPR experiments, although uMtCK recruited a higher number of binding sites on the membrane surface. However, it seems difficult to assess the individual contributions of hydrophobic and electrostatic interactions with respect to the observed binding affinities and kinetics. Site-directed mutagenesis studies of this region will help to further elucidate the interaction mode between MtCK and the mitochondrial membranes.

CONCLUSION

The presented structure confirms the high overall similarity of three-dimensional fold and active site conformation of all known CK isoenzymes. However, distinct structural features provide a molecular explanation for the various isoform-specific properties, especially for the differences in octamer stability and membrane binding observed between ubiquitous and sarcomeric MtCK. Concerning the critical role of MtCK in numerous diseases, the structure of ubiquitous MtCK isoform of human origin provides valuable information for future experiments.

ACKNOWLEDGMENTS

We thank A.W. Strauss and Z. Khuchua for providing the cDNA clone of human uMtCK and S. Eschenburg for helpful discussions and for carefully reading the manu-

script. Grant sponsor is Swiss National Science Foundation (number 3100-5082.97) to T.W. and U.S.

REFERENCES

- Wallimann T, Wyss M, Brdiczka D, Nicolay K, Eppenberger HM. Intracellular compartmentation, structure and function of creatine kinase isoenzymes in tissues with high and fluctuating energy demands: The "phosphocreatine circuit" for cellular energy homeostasis. *Biochem J* 1992;281:21–40.
- Wyss M, Smeitink J, Wevers RA, Wallimann T. Mitochondrial creatine kinase: a key enzyme of aerobic energy metabolism. *Biochim Biophys Acta* 1992;1102:119–166.
- Schlattner U, Forstner M, Eder M, Stachowiak O, Fritz-Wolf K, Wallimann T. Functional aspects of the X-ray structure of mitochondrial creatine kinase: a molecular physiology approach. *Mol Cell Biochem* 1998;184:125–140.
- Mühlebach SM, Gross M, Wirz T, Wallimann T, Perriard J-C, Wyss M. Sequence homology and structure predictions of the creatine kinase isoenzymes. *Mol Cell Biochem* 1994;133/134:245–262.
- Stachowiak O, Schlattner U, Dolder M, Wallimann T. Oligomeric state and membrane binding behavior of creatine kinase isoenzymes: implications for cellular function and mitochondrial structure. *Mol Cell Biochem* 1998;184:141–154.
- Schnyder T, Engel A, Lustig A, Wallimann T. Native mitochondrial creatine kinase (Mi-CK) forms octameric structures. II. Characterization of dimers and octamers by ultracentrifugation, direct mass measurement by STEM and image analysis of single Mi-CK octamers. *J Biol Chem* 1988;263:16954–16962.
- Marcellat O, Goldschmidt D, Eichenberger D, Vial C. Only one of the two interconvertible forms of mitochondrial creatine kinase binds to heart mitoplasts. *Biochim Biophys Acta* 1987;890:233–241.
- Schlegel J, Wyss M, Eppenberger HM, Wallimann T. Functional studies with the octameric and dimeric form of mitochondrial creatine kinase. Differential pH-dependent association of the two oligomeric forms with the inner mitochondrial membrane. *J Biol Chem* 1990;265:9221–9227.
- Rojo M, Hovius R, Demel R, Wallimann T, Eppenberger HM, Nicolay K. Interaction of mitochondrial creatine kinase with model membranes. A monolayer study. *FEBS Lett* 1991;281:123–129.
- Schlattner U, Wallimann T. A quantitative approach to membrane binding of human ubiquitous mitochondrial creatine kinase. *J Biomembr Bioenerg* 2000 (in press).
- Jacobus WE. Respiratory control and the integration of heart high-energy phosphate metabolism by mitochondrial creatine kinase. *Annu Rev Physiol* 1985;47:707–725.
- Crompton M. The mitochondrial permeability transition pore and its role in cell death. *Biochem J* 1999;341:233–249.
- O'Gorman E, Beutner G, Dolder M, Koretsky AP, Brdiczka D, Wallimann T. The role of creatine kinase in inhibition of mitochondrial permeability transition. *FEBS Lett* 1997;414:253–257.
- Khuchua ZA, Qin W, Boero J, Cheng J, Payne RM, Saks VA, Strauss AW. Octamer formation and coupling of cardiac sarcomeric mitochondrial creatine kinase are mediated by charged N-terminal residues. *J Biol Chem* 1998;273:22990–22996.
- Schlegel J, Zurbriggen B, Wegmann G, Wyss M, Eppenberger HM, Wallimann T. Native mitochondrial creatine kinase (Mi-CK) forms octameric structures. I. Isolation of two interconvertible Mi-CK isoforms: Dimeric and octameric Mi-CK. *J Biol Chem* 1988;263:16942–16953.
- Soboll S, Brdiczka D, Jahnke D, Schmidt A, Schlattner U, Wendt S, Wyss M, Wallimann T. Octamer-dimer transitions of mitochondrial creatine kinase in heart disease. *J Mol Cell Cardiol* 1999;31:857–866.
- Stachowiak O, Dolder M, Wallimann T, Richter C. Mitochondrial creatine kinase is a prime target of peroxynitrite-induced modification and inactivation. *J Biol Chem* 1997;273:16694–16699.
- Yuan G, Kaneko M, Masuda H, Hon RB, Kobayashi A, Yamazaki N. Decrease in heart mitochondrial creatine kinase activity due to oxygen free radical. *Biochem Biophys Acta* 1992;1140:78–84.
- Klivenyi P, Ferrante RJ, Matthews RT, Bogdanov MB, Klein AM, Andreassen OA, et al. Neuroprotective effects of creatine in a transgenic animal model of amyotrophic lateral sclerosis. *Nat Med* 1999;5:347–350.
- Beal MF. Mitochondrial dysfunction in neurodegenerative diseases. *Biochim Biophys Acta* 1998;1366:211–223.
- Pratt R, Vallis LM, Lim CW, Chisnall WN. Mitochondrial creatine kinase in cancer patients. *Pathology* 1987;19:162–165.
- Bergnes G, Yuan W, Khandekar VS, O'Keefe MM, Martin KJ, Teicher BA, Kaddurah-Daouk R. 1996. Creatine and phosphocreatine analogs: anticancer activity and enzymatic analysis. *Oncology Res* 1996;8:121–130.
- Schnyder T, Cyrklaff M, Fuchs K, Wallimann T. Crystallization of mitochondrial creatine kinase on negatively charged lipid layers. *J Struct Biol* 1994;112:136–147.
- Fritz-Wolf K, Schnyder T, Wallimann T, Kabsch W. Structure of mitochondrial creatine kinase. *Nature* 1996;381:341–345.
- Rao JK, Bujacz G, Wlodawer A. Crystal structure of rabbit muscle creatine kinase. *FEBS Lett* 1998;439:133–137.
- Eder M, Schlattner U, Becker A, Wallimann T, Kabsch W, Fritz-Wolf K. Crystal structure of brain-type creatine kinase at 1.41 Å resolution. *Protein Sci* 1999;8:2258–2269.
- Zhou G, Somasundaram T, Blanc E, Parthasarathy G, Ellington WR, Chapman MS. Transition state structure of arginine kinase: implications for catalysis of bimolecular reactions. *Proc Natl Acad Sci USA* 1998;95:8449–8454.
- Haas RC, Strauss AW. Separate nuclear genes encode sarcomere-specific and ubiquitous human mitochondrial creatine kinase isoenzymes. *J Biol Chem* 1990;265:6921–6927.
- Furter R, Kaldis P, Furter-Graves EM, Schnyder T, Eppenberger HM, Wallimann T. Expression of active octameric cardiac mitochondrial creatine kinase in *Escherichia coli*. *Biochem J* 1992;288:771–775.
- Bradford MM. A rapid and sensitive method for the quantitation of microgram quantities of protein utilizing the principle of protein-dye binding. *Anal Biochem* 1976;72:248–254.
- Wallimann T, Turner DC, Eppenberger HM. Localization of creatine kinase isoenzymes in myofibrils. *J Cell Biol* 1995;75:297–317.
- Kabsch W. Evaluation of single-crystal X-ray diffraction data from a position-sensitive detector. *J Appl Cryst* 1988;21:916–924.
- Kabsch W. Automatic processing of rotation diffraction data from crystals of initially unknown symmetry and cell constants. *J Appl Cryst* 1993;26:795–800.
- Rossmann MG. The molecular replacement method. New York: Gordon and Breach; 1972. 267 p.
- Brünger AT, Adams PD, Clore GM, et al. Crystallography & NMR System (CNS): a new software system for macromolecular structure determination. *Acta Cryst D* 1998;54:905–921.
- Brünger AT. Free R value: a novel statistical quantity for assessing the accuracy of crystal structures. *Nature* 1992;355:472–475.
- Engh RA, Huber R. Accurate bond and angle parameters for X-ray protein structure refinement. *Acta Crystallogr A* 1991;47:392–400.
- Read RJ. Improved Fourier coefficients for maps using phases from partial structures with errors. *Acta Crystallogr A* 1986;42:140–149.
- Rice T, Brünger AT. Torsion angle dynamics: reduced variable conformational sampling enhances crystallographic structure refinement. *Proteins* 1994;19:277–290.
- Brünger AT. Crystallographic refinement by simulated annealing. Application to a 2.8 Å structure of aspartate aminotransferase. *J Mol Biol* 1988;203:803–816.
- Brünger AT, Adams PD, Rice LM. New applications of simulated annealing in X-ray crystallography and solution NMR. *Structure* 1997;5:325–336.
- Laskowski RA, MacArthur MW, Moss DS, Thornton JM. PROCHECK: a program to check the stereochemical quality of protein structures. *J Appl Cryst* 1993;26:283–291.
- Ramakrishnan C, Ramachandran GN. Stereochemical criteria for polypeptide and protein chain conformations. II. Allowed conformations for a pair of peptide units. *Biophys J* 1965;5:909–933.
- Kabsch W, Sander C. Dictionary of protein secondary structure: Pattern recognition of hydrogen-bonded and geometrical features. *Biopolymers* 1983;22:2577–2637.
- Gross M, Lustig A, Wallimann T, Furter R. Multiple-state equilibrium unfolding of guanidino kinases. *Biochemistry* 1995;34:10350–10357.

46. Gross M, Furter-Graves EM, Wallimann T, Eppenberger HM, Furter R. 1994. The tryptophan residues of mitochondrial creatine kinase: Roles of Trp-223, Trp-206, and Trp-264 in active-site and quaternary structure formation. *Protein Sci* 1994;3:1058–1068.
47. Milner-White EJ, Watts DC. Inhibition of adenosine 5'-triphosphate-creatine phosphotransferase by substrate-anion complexes. Evidence for the transition-state organization of the catalytic site. *Biochem J* 1971;122:727–740.
48. Ellington WR, Roux K, Pineda AO. Origin of octameric creatine kinases. *FEBS Lett* 1998;425:75–78.
49. Cheneval D, Carafoli E, Powell GL, Marsh D. A spin-label electron spin resonance study of the binding of mitochondrial creatine kinase to cardiolipin. *Eur J Biochem* 1989;186: 415–419.
50. Vacheron MJ, Clottes E, Chautard C, Vial C. Mitochondrial creatine kinase interaction with phospholipid vesicles. *Arch Biochem Biophys* 1997;344:316–324.
51. Diederichs K, Karplus PA. Improved R-factors for diffraction data analysis in macromolecular crystallography. *Nat Struct Biol* 1997;4:269–275.
52. Jones TA, Zou J-Y, Cowan SW, Kjeldgaard M. Improved methods of building protein models in electron density maps and the location of errors in these models. *Acta Crystallogr A* 1991;47:110–119.